

Background

Hepatocytes apoptosis, the hallmark of NASH, contributes to liver injury and fibrosis. Although, both the intrinsic and extrinsic apoptotic pathways are involved in the pathogenesis of NASH, the final common step of apoptosis is executed by a family of cysteine proteases termed caspases. In particular, the effectors caspases are known to be activated in NASH. These caspases dismantle the cell generating apoptotic bodies. Furthermore, these apoptotic cell can stimulates hepatic stellate cells (HSC), leading to their activation and fibrogenesis.

Aim

Our aim was to ascertain if the administration of PF-03491390, a pan-caspase inhibitor, ameliorates liver injury and fibrosis in a murine model of NASH.

Questions

- Does the pan-caspase inhibitor ...
- 1) attenuate hepatocyte apoptosis and liver injury?
 - 2) reduce hepatic steatosis?
 - 3) decrease hepatic inflammation?
 - 4) inhibit HSC activation and attenuate hepatic fibrosis?

Experimental Approach

Animals: C57BL/6J mice (3-4 mo old) were fed regular chow (Reg Chow) or high fat diet (HFD) for 20 weeks. All mice were treated with vehicle or pan-caspase inhibitor PF-03491390 PO (0.3mg/kg/day).

Apoptosis: Hepatocyte apoptosis was assessed by TUNEL assay. Caspase activity was assessed by biochemical measurement of Caspase-3 activity and immunoblot for PARP protein.

Liver Injury: Liver injury was evaluated by histopathology (H&E staining) and serum transaminases (ALT and AST).

Hepatic Steatosis: Steatosis was measured by liver triglyceride content and by histopathology (H&E staining).

Hepatic Inflammation: Inflammation was evaluated by histopathology score (H&E staining) and qPCR for Interleukin-1beta (IL-1β).

HSC Activation: HSC activation was measured by immunofluorescence (IF) and qPCR for alpha-smooth muscle actin (αSMA).

Liver Fibrosis: Liver fibrosis was evaluated by histopathologic score (Mallory Trichrome), Sirius Red staining and qPCR for Collagen 1 (Col-1).

Statistical Analysis: Data are mean ± SEM. One-way analysis of variance (ANOVA) was utilized with post-hoc Student-Newman-Keuls test to correct for multiple comparisons, and significance was accepted at p<0.05.

Figure 1. Hepatocyte apoptosis and caspase activation are attenuated in PF-03491390 treated HFD-fed mice

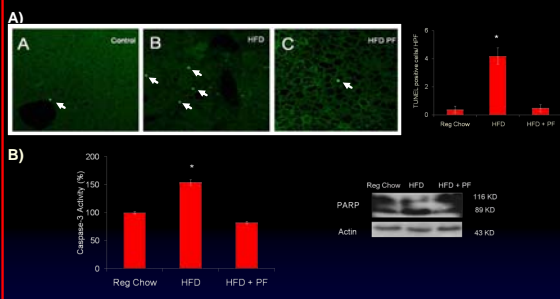


Figure 1. (A) The number of TUNEL-positive cells (marked with arrows) was quantitated and expressed as apoptotic cells/10 high-power fields (HPF). Data are from eight independent animals per group and are expressed as the mean ± standard error. (B) Apoptosis was also evaluated by measuring caspase-3 biochemical activity (Percentage of activity from Reg Chow mice) and by immunoblot of PARP 1/2 cleavage (During apoptosis full-length 116KD PARP protein is cleaved by caspase-3 into an 89KD fragment). Representative immunoblot from each animal group is shown. Data points represent experiments from six independent animals, and bars are expressed as the mean ± standard error. *p<0.05. **Regular Chow-fed mice (Reg Chow), High Fat Diet-fed mice (HFD) and PF-02491390 treated High Fat Diet-fed mice (HFD + PF)**

Figure 2. Liver injury is reduced in PF-03491390 treated HFD-fed mice

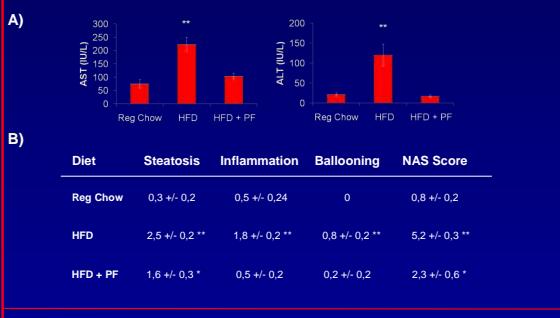


Figure 2. (A) Serum AST and ALT values were measured. Data are from eight independent animals and are expressed as the mean ± standard error. (B) Liver injury was quantified using the NAS (Non-alcoholic fatty liver disease Activity Score) histological score. Data are from nine independent animals and are expressed as the mean ± standard error. *p<0.05, **p<0.001 **Regular Chow-fed mice (Reg Chow), High Fat Diet-fed mice (HFD) and PF-02491390 treated High Fat Diet-fed mice (HFD + PF)**

Figure 3. Liver steatosis and serum metabolic derangements are not reduced in PF-03491390 treated HFD-fed mice

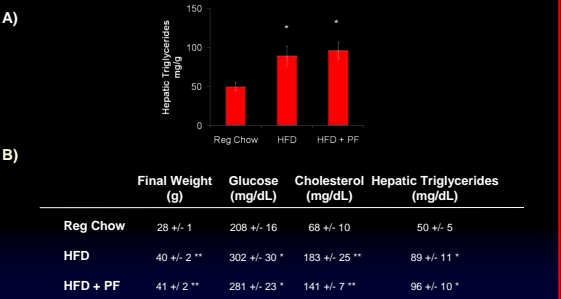


Figure 3. (A) Hepatic triglycerides content in the livers were measured. Data are from six independent animals per group and are expressed as the mean ± standard error. (B) Body weights, serum glucose and cholesterol (indices of metabolic derangements and insulin resistance) were measured. Data are from six independent animals and are expressed as the mean ± standard error. *p<0.05, **p<0.001 **Regular Chow-fed mice (Reg Chow), High Fat Diet-fed mice (HFD) and PF-02491390 treated High Fat Diet-fed mice (HFD + PF)**

Figure 4. Liver inflammation is decreased in PF-03491390 treated HFD-fed mice

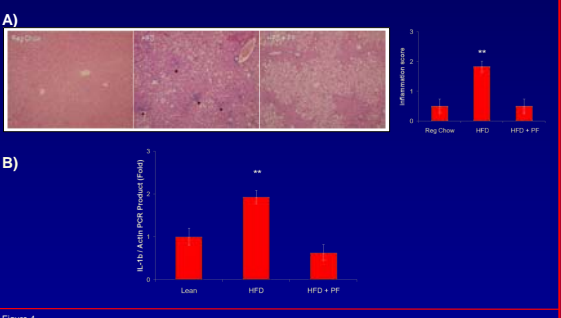


Figure 4. (A) Representative photomicrographs of conventional H&E-stained liver sections (magnification 20X) are shown. Inflammatory foci are marked with dark asterisks. Inflammatory foci were quantified using NAS histological score. Data are from nine independent animals and are expressed as the mean ± standard error. (B) Interleukin-1beta (IL-1β), a marker of hepatic inflammation, was quantitated using real-time PCR technology (qPCR). The expression was normalized as a ratio using beta-Actin (Actin) as a housekeeping RNA. Data are from six independent animals and are expressed as the mean ± standard error. *p<0.05, **p<0.001.

Figure 5. HSC Activation and liver fibrogenesis are attenuated in PF-03491390 treated HFD-fed mice

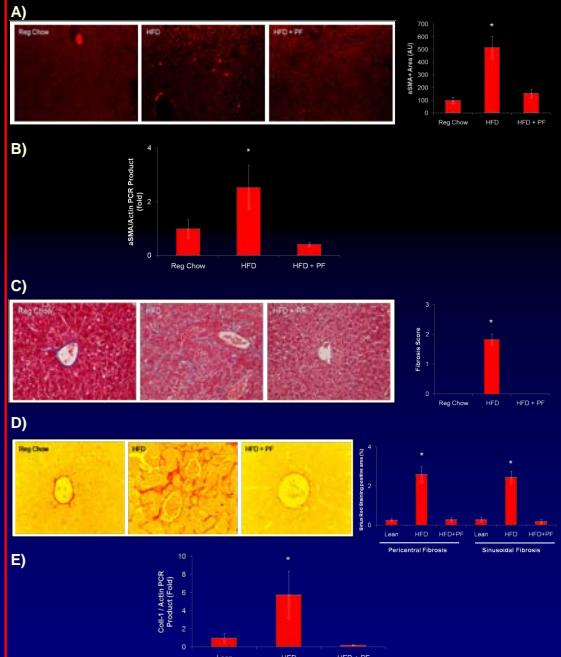


Figure 5. (A) Representative photomicrographs after immunofluorescence for αSMA (left) are depicted (magnification 40X), quantification of αSMA+ area is shown (right). (B) αSMA mRNA expression, marker of HSC activation, was quantified using real-time PCR technology (qPCR). (C) Representative photomicrographs of Mallory's trichrome-stained (left) liver sections (magnification 40X) are shown. Fibrosis was quantified using modified NAS histological score (right). (D) Sirius red staining, a chemical stain of collagen deposition in the liver, was performed. Collagen fibers stained with Sirius red were quantitated using digital image analysis in pericentral and sinusoidal areas (right). Representative photomicrographs of liver sections (left) are depicted (magnification 400X). (E) Collagen 1 (Col-1) mRNA expression, marker of hepatic fibrogenesis, was quantified using real-time PCR technology (qPCR). Data are from five-nine independent animals and are expressed as the mean ± standard error. *p<0.05, **p<0.001.

Conclusion

Collectively, these data demonstrate that in a murine model of NASH, liver injury and fibrosis are suppressed by inhibiting hepatocytes apoptosis and suggests that PF-03491390 may be an attractive anti-fibrotic therapy in NASH